

***d*-wave, dimer, and chiral states in the two-dimensional Hubbard model**

Alberto Parola and Sandro Sorella

International School for Advanced Studies (SISSA), Strada Costiera 11, Trieste, Italy

Michele Parrinello

*International School for Advanced Studies (SISSA), Strada Costiera 11, Trieste, Italy
and IBM Research Division, Zurich Research Laboratory, 8803 Rüschlikon, Switzerland*

Erio Tosatti

International School for Advanced Studies (SISSA), Strada Costiera 11, Trieste, Italy

(Received 21 June 1990)

The ground-state properties of two holes on a 4×4 Hubbard cluster have been studied using a Lanczos algorithm at intermediate coupling $U=4$. Several states have been found to lie within a very small energy range at the bottom of the spectrum. Although many properties of these states are remarkably similar, their overall symmetries are quite different, suggesting different possible scenarios in larger systems.

The 2D Hubbard model, and the related t - J model, are presently hoped to provide insight into the behavior of the high- T_c Cu-O superconductors.¹ For a square lattice at zero doping, antiferromagnetism prevails for all values of U . However, in the region of small doping, more relevant to Cu-O superconductors, much less information is available. Several authors using different theoretical methods have suggested the possible existence of many interesting phases: resonating-valence-band (RVB) flux phases,² chiral phases,³ dimer phases,⁴ and nonuniform phases.²

In this Brief Report we show, by detailed analysis of a small size system, namely, a 16-site (4×4) Hubbard lattice with 14 electrons, that very interesting information on these possible ground states is foreshadowed by the properties of the low-lying states of the two-hole problem. In particular, we find three uniform and one density-wave state within a very small energy difference of one another. Among the possible uniform states, one closely resembles a dimer phase while another can be interpreted as a kind of flux phase, or chiral spin liquid. We also find that all these and exclusively these low-lying states can be given an approximate representation in terms of linear combinations of "Fermi-level" hole creation operators acting onto the half-filled ground state. This form suggests new approximate wave functions for the 2D Hubbard model at small but finite doping.

We seek the lowest eigenvalues of the 4×4 Hubbard model with periodic boundary conditions by a power method supplemented by a few Lanczos steps at the end in order to improve accuracy. This method, although rather slow, minimizes memory requirements which are at present the major limiting factor for this kind of calculation. Special coding of the wave function and memory access techniques were used to make the calculation feasible. In this calculation we have restricted our search to the subspace of $S_z=0$ and even total spin, whose size is

$M(M+1)/2$ where

$$M = \begin{pmatrix} N_{\text{sites}} \\ N_{\uparrow} \end{pmatrix}.$$

In the present case $N_s=16$, $N_{\uparrow}=7$, the size is 7×10^7 . No explicit use has been made of the spatial symmetries of the lattice. The initial vector ψ_T of our iterative procedure has been taken to be an appropriate *random* superposition of eigenvector of the total momentum. This device permits the simultaneous study of all possible symmetries and \mathbf{k} vectors. Each of them is singled out after convergence by using a symmetry projector. We find that all the low-lying state, within our even S manifold, are singlets. Convergence has been checked throughout, and all figures given below represent accurate results. In particular, accuracy in the energy is always better than one part in 10^6 . To our knowledge, this is the largest size computation ever carried out for this problem. A description of the method and some preliminary results can be found in Ref. 5.

In Table I we show the resulting energies for each total \mathbf{k} vector \mathbf{Q} along with the magnetic structure factor $S_{\text{mag}}(\pi, \pi)$, the density structure factor $S_{\text{den}}(\pi, \pi)$ the single-particle density matrix ρ_n (where n denotes the n th neighbor) and, where defined, the rotational symmetry of the state g . The energy improvement upon doping, which is seen by comparison with the undoped case in Table I, is basically a kinetic energy gain, as indicated also by ρ_1 . Although this is not surprising, it is interesting to note that the ground state does not have the best kinetic energy. Doping has a clear depressing effect on the magnetic $S_{\text{mag}}(\pi, \pi)$, but does not affect so much the density response at the same wave vector.

The ground state is threefold degenerate $(0,0)$, $[(0,\pi), (\pi,0)]$. This agrees well with the existing t - J model calculations.^{6,7} The extra, nonrotational, degeneracy between $(0,0)$ and $(0,\pi)$ is due to an additional symmetry of

TABLE I. Numerical results for the $U=4$ Hubbard model, see text.

ν	16/16			14/16			
\mathbf{Q}	(0,0)	(0,0)	(0, π)	(π,π)	($\pm\frac{\pi}{2},\pm\frac{\pi}{2}$)	($\pi,\frac{\pi}{2}$)	(0, $\pi/2$)
g	s	d		p			
E/N	-0.8514	-0.9840	-0.9840	-0.9839	-0.9839	-0.922	-0.922
E_{kin}/N	-1.3118	-1.3366	-1.3375	-1.3375	-1.3375	-1.24	-1.24
$S_{\text{mag}}(\pi,\pi)$	3.64	2.14	2.18	2.18	2.16		
$S_{\text{den}}(\pi,\pi)$	0.385	0.4242	0.4242	0.4245	0.4245		
ρ_1	0.164	0.167	0.168	0.167	0.167		
ρ_2	0.0	5.4×10^{-2}	-7.8×10^{-4}	-7.4×10^{-4}	-7.7×10^{-4}		
ρ_3	0.0	-5.6×10^{-2}	5.5×10^{-2}	5.4×10^{-2}	-7.4×10^{-4}		
ρ_4	-4.8×10^{-2}	-5.0×10^{-2}	-5.1×10^{-2}	-5.1×10^{-2}	-5.0×10^{-2}		
ρ_5	0.0	-5.1×10^{-2}	-5.1×10^{-2}	-5.1×10^{-2}	-5.1×10^{-2}		

the Hubbard Hamiltonian, specific to the 4×4 lattice. A new striking feature is the presence of extremely low-lying excited states with $(\pm\pi/2, \pm\pi/2)$ and at (π, π) . By contrast states at $(0, \pi/2), (\pi, \pi/2)$ are found to be much higher in energy. The density matrix indicates that electron hopping within the same sublattice, strictly forbidden by charge conjugation symmetry at half-filling, is allowed in a substantial amount in presence of holes.

We have also studied charge-charge and spin-spin correlation functions for all the low-lying states. Rather surprisingly we find that all the low-lying states have similar correlations. The spin correlations $c(\mathbf{R}) = \langle S_x(0)S_x(\mathbf{R}) \rangle$ all show evidence of a tendency toward antiferromagnetic ordering which is however substantially weakened with respect to the half-filled case [see Fig. 1 and also $S_{\text{mag}}(\pi, \pi)$ in Table I]. Remarkably, the hole-hole correlations $h(\mathbf{R}) = -1 + \langle h_0 h_{\mathbf{R}} \rangle / \langle h_0 \rangle^2$ (where $h_{\mathbf{R}} = \langle [1 - n^\uparrow(\mathbf{R})][1 - n^\downarrow(\mathbf{R})] \rangle$) are slightly “repulsive” and not much structured (Fig. 2), i.e., the two holes tend to stay apart in all cases. Previous $t-J$ model studies found a crossover between repulsion and attraction for increasing J , but seem to attach importance only to the attractive regime.⁶ In view of existing suggestions that long-range hole-hole correlations should show overall indifference if not repulsion¹ or instead attraction,⁸ it would be desirable to remove the short-range repulsion effects present in both pictures. If we take the undoped $h(\mathbf{R})$ as representative of these “bare” correla-

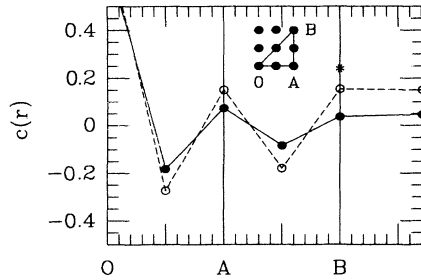


FIG. 1. Spin-spin correlations for $U=4$ along the path shown in the inset. Dashed line: half-filling. Solid line: two holes in the $(0,0)$ state. The asterisk represents the corresponding Heisenberg value on the same cluster.

tions then one would conclude (see Fig. 2) that the additional correlations are repulsive at short range but less so at the largest available distance. By contrast, very recent calculations indicate that two holes in the 4×4 lattice have a nonzero binding energy.⁹ This discrepancy suggests the presence of severe finite-size effects. Only a proper finite-size scaling will eventually be able to resolve the issue. The repulsive hole-hole correlations also imply that phase separation does not occur in this region of the phase diagram.

In order to extract more information we analyze in detail the nature of the low-lying states. If they are degenerate, a particular linear combination will be presented, based on physical motivations, such as the analogy with existing mean-field results.¹⁰

$(0,0)$: This state is even under x and y reflections and changes sign under $\pi/2$ rotation. Therefore the two holes are in a $d_{x^2-y^2}$ relative state. The symmetry of this state is the same as that of one of the proposed d -wave RVB states.

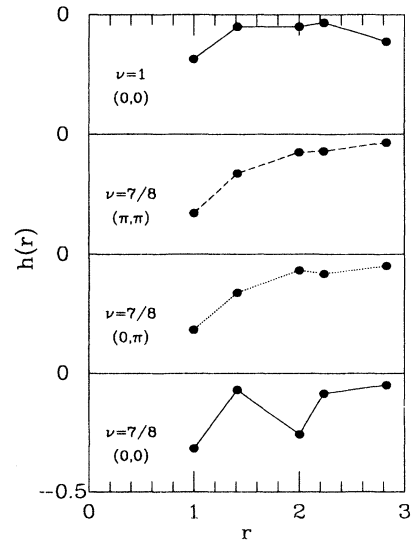


FIG. 2. Hole-hole correlations for half-filling and for the three uniform states at $\nu = \frac{7}{8}$. Note that the two holes tend to stay apart (repulsive correlations).

$(0, \pi); (\pi, 0)$: This doublet can be combined to break translational invariance, while restoring rotational symmetry. The states thus obtained exhibit neither charge- nor spin-density-wave spatial modulation. Rather, an order parameter distinguishing the two inequivalent states of the doublet can be identified as a *current fluctuation operator*: we find an interesting nonhomogeneous current pattern which can be identified by measuring $\langle \chi_{ij} \chi_{jk} \chi_{kl} \chi_{li} \rangle$, the circulation along the elementary square plaquettes of the operator $\chi_{ij} = \sum_{\sigma} c_i^{+\sigma} c_j^{\sigma}$. This gives 0.18 and -0.008 along two nonequivalent neighboring plaquettes. This result rather resembles the pattern one could expect for some superposition of *dimer* phases, as recently discussed by Dombre and Kotliar.⁴

$(\pm\pi/2, \pm\pi/2)$: This quartet of states can also be combined to give translationally noninvariant states with a uniaxial symmetry analogous to the “kite” phase of Affleck and Marston.² One thus finds two pairs of states characterized by a weak CDW ($\Delta n/n = 6.5 \times 10^{-3}$) arranged to form a two-sublattice structure. Another feature of this state is the weak asymmetry between $\langle \chi_{i,j} \rangle$ at opposite kite sides: $\langle \chi_{i,i+x} \rangle = \langle \chi_{i,i-y} \rangle = 0.3340$, $\langle \chi_{i,i+y} \rangle = \langle \chi_{i,i-x} \rangle = 0.3347$.

(π, π) : This is a doublet of translationally invariant states with p -like rotational symmetry. The circularly polarized combinations $p_x \pm ip_y$ have well-defined chiralities. Therefore this state is a natural candidate for a finite-size realization of a “chiral spin liquid.” Notice that in such a homogeneous and isotropic state, no net current can flow on the bonds of the lattice, unlike the picture envisaged by Rice *et al.*¹¹ We have investigated the circulation dependence on the plaquette area. For a long-range chiral ordered state of the type proposed by Wen, Wilczek, and Zee,³ the phase of the circulation should increase with the area. The flux states first introduced by Affleck and Marston and by Kotliar² imply $\frac{1}{2}$ flux quantum per electron. The phase of a flux state is predicted to depend upon doping in the simple manner $\phi = \nu \pi A$. The results for our (π, π) state given in Fig. 3 do show an increase of phase with the plaquette area which compares rather well, though not exactly, with the flux state values. This state is characterized by a nonzero chiral order parameter: $\langle P(R) \rangle = \langle \mathbf{S}_i \cdot \mathbf{S}_j \times \mathbf{S}_k \rangle = 1.3 \times 10^{-2}$, where i, j, k label the vertices of the elemen-

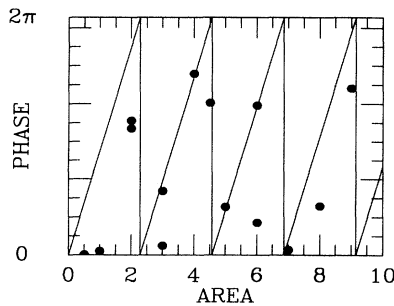


FIG. 3. Phases associated with several plaquettes of different areas (●) as found in the (π, π) chiral state. The phase expected for a flux state with $\frac{1}{2}$ flux per electron is also shown (solid line).

tary triangle centered at R . This provides a first indication of the rather small amount of *parity symmetry breaking* to be expected for a Hubbard model as opposed to the more “ad hoc” Hamiltonians.¹² If, as it may seem possible, the chiral long-range order still shows up in the thermodynamic limit, then statistical transmutation would necessarily follow.³

This exhausts the set of low-lying states of the two holes. It seems remarkable that, in spite of the obvious size limitation, so many different kinds of states already show up in the two-holes problem. It is clearly desirable at this stage to have a simple description and rationalization of these states. A crucial clue is provided by the change in the momentum distribution function $n(k)$ which we observe upon doping. As exemplified in the $(0, 0)$ case

$$\delta n(k) = n(k)|_{\nu=16/16} - n(k)|_{\nu=14/16}$$

shown in Fig. 4 is a very strongly peaked function at $(0, \pi)(\pi, 0)$ suggesting that the main ingredients in this state are two holes at these \mathbf{k} vectors. This turns out to be a general property for all the low-lying states. For all of them, the true eigenfunction can, approximately but accurately, be described by the form

$$|\psi_{N/2-2}\rangle = \sum_{\mathbf{k}_1, \mathbf{k}_2} \phi(\mathbf{k}_1, \mathbf{k}_2) c_{\mathbf{k}_1}^\dagger c_{\mathbf{k}_2}^\dagger |\psi_{N/2}\rangle, \quad (1)$$

where $|\psi_{N/2}\rangle$ is the half-filled ground state. The form of $\phi(\mathbf{k}_1, \mathbf{k}_2)$ is uniquely determined by the following requirements: (i) \mathbf{k}_1 and \mathbf{k}_2 should lie on the outermost shell of the $U=0$ Fermi surface at half-filling, (ii) $\mathbf{k}_1 + \mathbf{k}_2$ should equal the total momentum of the state, (iii) the holes form a singlet state, (iv) the holes cannot sit on the same site. The latter two requirements prevent the holes from being in a relative s -like state [i.e., $\phi(r_1=r_2)=0$]. Although very simple, the wave functions (2) reproduce very well the properties of all the true low-lying states. It is to be noted that most of the correlations in $|\psi_{(N/2)-2}\rangle$ derive from those already present in the parent half filled-state $|\psi_{N/2}\rangle$.

For the 4×4 lattice the Fermi surface consists of 6 points $(\pm\pi/2, \pm\pi/2), (0, \pi), (\pi, 0)$. Out the 36 two-hole states that can be formed, 15 are triplets and 21 singlets.

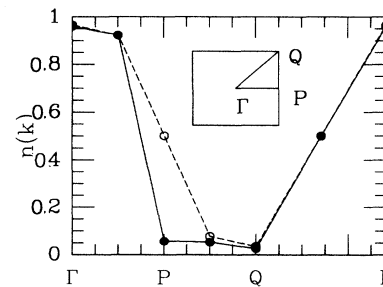


FIG. 4. Momentum distribution $n(k)$ for the two-hole state $(0, 0)$ (●) as compared with the half-filled, zero-hole, state (○).

Out of the latter, 10 states satisfy the above criteria. We find that nine of them are good approximations to the low-lying states described above, as anticipated¹³

The above analysis shows how to build approximate but accurate, two-hole states, starting from the knowledge of the ground state at half-filling. It seems possible, although clearly speculative, at this stage, to generalize this result to the many-hole, dilute limit. One such generalized wave function could be, for example,

$$\Psi = \exp \left[\sum_{\mathbf{k}_1, \mathbf{k}_2} \phi(\mathbf{k}_1, \mathbf{k}_2) c_{\mathbf{k}_1}^\dagger c_{\mathbf{k}_2}^\dagger \right] |\psi_{N/2}\rangle, \quad (2)$$

where the pair envelope function $\phi_{\mathbf{k}_1, \mathbf{k}_2}$ can be determined variationally, but must obey the same rules as described above for two holes. The richness of different states found in a tiny range of energy suggests that in the infinite-size limit various scenarios are indeed possible. Translational invariance (charge and spin uniformity) is equivalent to requiring $k_1 + k_2 = \mathbf{Q} = \mathbf{G}/2$, where \mathbf{G} is a reciprocal lattice vector. The symmetry of $\phi(\mathbf{k}_1, \mathbf{k}_2)$ will of course be reflected in the overall symmetry of the corresponding Ψ . We do not yet know, however, any other property of these proposed states, including the possible presence of off-diagonal long-range order. We note, however, a certain similarity of our wave function (3) with the spin-bag picture by Schrieffer *et al.*,⁸ which is recovered, in particular, if $|\psi_{N/2}\rangle$ is approximated by a spin-density wave state and $\phi(\mathbf{k}_1, \mathbf{k}_2)$ is peaked around pockets at the corners of the Fermi surface.

By a direct extension of our two-hole states, an explicit choice of $\phi(\mathbf{k}_1, \mathbf{k}_2)$ which leads to a many-hole state with

explicitly broken chirality is

$$\phi(\mathbf{k}_1, \mathbf{k}_2) = \sum_{\alpha, \beta = \pm 1} \beta e^{-i(\pi/4)\alpha\beta} f_{\alpha, \beta}(\mathbf{k}_1) f_{\alpha, \beta}(\mathbf{k}_2),$$

where $\mathbf{k}_2 = \mathbf{Q} - \mathbf{k}_1$, $\mathbf{Q} = (\pi, \pi)$ and $f_{\alpha, \beta}$ is a function peaked about $(\alpha\pi/2, \beta\pi/2)$. Alternatively, the choice

$$\phi(\mathbf{k}_1, \mathbf{k}_2) = \sum_{\alpha, \beta = \pm 1} \beta f_{\alpha, \beta}(\mathbf{k}_1) f_{-\alpha, \beta}(\mathbf{k}_2)$$

$\mathbf{k}_2 = \mathbf{Q}' - \mathbf{k}_1$, [$\mathbf{Q}' = (0, \pi)$], represents a ‘‘dimer’’ state. Finally

$$\phi(\mathbf{k}_1, \mathbf{k}_2) = g_x(\mathbf{k}_1)g_x(\mathbf{k}_2) - g_y(\mathbf{k}_1)g_y(\mathbf{k}_2),$$

where $\mathbf{k}_2 = -\mathbf{k}_1$, $g_x(\mathbf{k})$ [$g_y(\mathbf{k})$] is peaked near $(\pi, 0)$ [$(0, \pi)$], yields a d -wave state. A study of the properties of these states is under way.

In summary, we have presented a detailed study of the two-hole problem in the 2D Hubbard model, which uncovers a manifold of ground states (or very nearly ground states) including a d -wave state, a dimerlike state, and a chiral flux state. From these exact states, approximate wave functions are constructed which permit extension to the thermodynamic limit.

We are grateful to S. Baroni and R. Car for their help and to J. R. Schrieffer for discussions. We acknowledge support from the SISSA-CINECA collaborative project, under the sponsorship of the Italian Ministry of Scientific Research, the National Institute for Physics of Matter (INFM), and also (E.T.) from the European Research Office, U.S. Army.

¹See, for instance, P. W. Anderson, *Frontiers and Borderlines in Many Particles Physics* (North-Holland, Amsterdam, 1988).

²I. Affleck and J. B. Marston, *Phys. Rev. B* **37**, 3774 (1988); G. Kotliar, *ibid.* **37**, 3664 (1988).

³X. G. Wen, F. Wilczek and A. Zee, *Phys. Rev. B* **39**, 11413 (1989); G. Baskaran (unpublished).

⁴S. A. Kivelson, D. S. Rokhsar, and J. P. Sethna, *Phys. Rev. B* **35**, 8865 (1987); T. Dombre and G. Kotliar, *ibid.* **39**, 855 (1989).

⁵A. Parola *et al.*, *Int. J. Mod. Phys. B* **3**, 1865 (1989).

⁶J. Bonča, P. Prelovsek, and I. Sega, *Phys. Rev. B* **39**, 7074 (1989).

⁷Y. Hasegawa and D. Poilblanc, *Phys. Rev. B* **40**, 9035 (1989); E. Dagotto, J. R. Schrieffer, A. Moreo, and T. Barnes (unpublished).

⁸J. R. Schrieffer, X. G. Wen, and S. C. Zhang, *Phys. Rev. B* **39**, 11 663 (1989).

⁹E. Dagotto *et al.*, *Phys. Rev. B* **41**, 811 (1990); G. Fano *et al.*, *ibid.* **42**, 6877 (1990).

¹⁰An alternative, but exactly equivalent, presentation of the same information could have been obtained abandoning pure states in favor of density-matrix averages in the $T \rightarrow 0$ limit.

¹¹P. Lederer, D. Poilblanc, and T. M. Rice, *Phys. Rev. Lett.* **63**, 1519 (1989).

¹²We have also studied the spatial correlations $\langle P(0)P(R) \rangle$, and found them still large, of order 10^{-2} for the largest distance in the cluster ($R = \sqrt{8}$). Note that the $R \rightarrow \infty$ value would be $(\langle P(0) \rangle)^2 = 1.7 \times 10^{-4}$.

¹³The tenth state has $k = (0, 0)$ and it has symmetric d_{xy} combination of holes $(\pm\pi/2, \pm\pi/2)$. A state of this symmetry has been found among the excited states at a considerably higher energy ($\Delta E \sim 0.3t$). However we found it impossible to represent as in Eq. (1).